eISSN: 2976-1190

Journal of Engineering and Sciences

Vol. 4 Issue 1 May 30, 2025
DOI:10.3126/jes2.v4i1.70754
Journal homepage: Journal of Engineering and Sciences (nepjol.info)
Publisher: Research Management Cell, Pashchimanchal Campus, Lamachour, Pokhara

Debris Flow Analysis and Susceptibility Mapping Using Flow-R

Anish Aryal[1*], Binod Bohara[2], Tulasi Ram Bhattarai[3], Asmita Aryal[4]
[1]*TAC Hydro Consultancy Private Limited, Lalitpur, Nepal*
[2]*Department of Civil Engineering, IOE Pashchimanchal Campus, Tribhuvan University, Nepal*
[3]*Ministry of Urban Development, Kathmandu, Nepal*
[4]*Department of Graduate Studies, Nepal College of Information Technology, Pokhara University, Nepal*
**Corresponding Email: anisharyal35@gmail.com*
(Manuscript Received: 24/10/2025; Revised: 19/05/2025; Accepted: 21/05/2025)

Abstract

Debris flow poses a significant challenge, mostly in hilly areas of Nepal. Despite the frequency and devastation caused by such events, accurately predicting debris flow paths and their impact remains a major difficulty. The present study addresses this critical problem by utilizing the Flow-R model, an empirical, open-source tool ideal for constrained resources. Through debris flow modelling and hazard mapping, this study investigates the Ramtola landslide area located in Baglung Municipality. A combination of methods is employed, including Flow-R path prediction, field-based susceptibility mapping, and GIS-based analysis. By integrating these three approaches, this study provides a relatively accurate assessment of debris flow hazard. The results demonstrate that this comprehensive methodology can significantly enhance risk evaluation and mitigation strategies in debris flow-prone areas.

Keywords: Flow-R; Debris flow analysis; Spreading algorithms; Susceptibility maps.

1 Introduction

Debris flows are one of the most common geological hazards in the Nepal Himalaya, taking many lives and homes each year. It can be defined as a surge of sediment materials, mud, stones, and other debris, primarily in the mountain regions with high slopes (Du et al., 2021); (Hungr et al., 2014). In Nepal, Debris flows occur often in areas with loose slope-forming materials (Dahal et al., 2006). Debris flows are differentiated by speed and turbulence, with steep channels or slopes exhibiting high flow rates.

Landslide susceptibility mapping is a method for identifying and mapping areas prone to Debris Flow. Landslide susceptibility mapping entails examining various characteristics that influence the beginning and course of landslides and combining them into a geographical model (Vianello et al., 2023). The elements that affect a given area's susceptibility to landslides, such as altitude, geology, soil type, land use, slope, and distance to drainage, must be determined.

Both qualitative (inventory-based and knowledge-driven approaches) and quantitative (data-driven methods and physically based models) methodologies can be used to evaluate the susceptibility of landslides (Vianello et al., 2023). The risk of landslides in the Himalayan landscape is predicted to grow in the future, owing to the climate change phenomenon (Xu et al., 2022). In that context, it is necessary to properly identify the location, propagation, and deposition amount of the debris from a few events, and promote reliable hazard and risk evaluation.

This study uses the Flow-R model to map landslide susceptibility and assess debris flow propagation paths. Therefore, it aims to analyze landslide patterns and provide a susceptibility map of hilly regions by integrating Flow-R, flow-based maps, and a GIS-based approach. The Ramtola landslide, located at Baglung Municipality in the hilly region of Nepal, serves as a case study.

2 Study Area

This area lies in the middle hills of Nepal among three geographical regions: the High Himalayas, the Middle Mountains, and the Terai, as shown in Figure 1. A total of 16% of the land area of Nepal is covered by high mountains, which includes eight high peaks that are among the 14 highest peaks in the world. The height of the middle hills ranges from 500 to 3000 m, and this zone covers 67% of the total land area of the country, while the lowest plains area accounts for 17%. The study area represents the middle hills (67%) of Nepal, which are densely populated and prone to debris flow. The study area represents the Middle Mountains in which the residents are vulnerable due to living in their homes, working in the fields, or walking around debris flow-prone areas. This study area is located within Latitude 28° 10' 00'' N to 28° 15' 00 ''N and Longitude 83° 30' 00'' E to 83° 40' 00'' E.

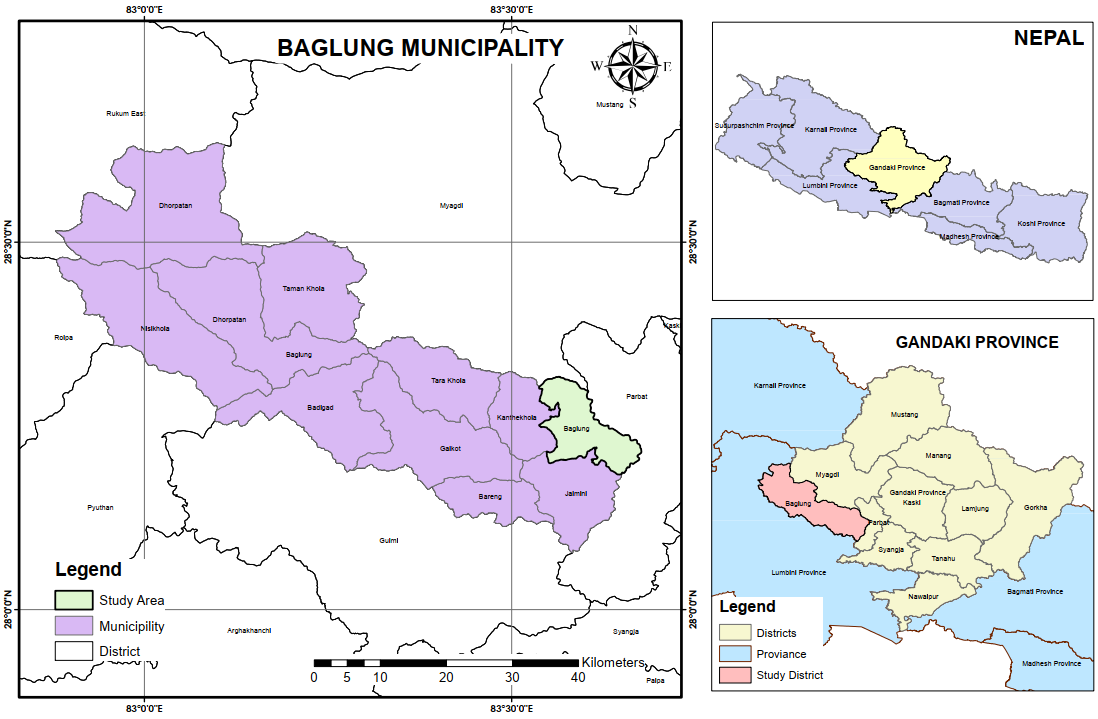

Figure 1: Location of the study area

2.1 Geological Setting

The study area lies in the Kushma Formation, consisting of greenish grey, white fine to medium grained at places, ripple-marked massive quartzites intercalated with green phyllites and amphibolite at a few places.

The study area of Ward-11 in Baglung Municipality was selected because of the numerous ongoing debris falls in the region. Geologically, the area is very weak & fragile, and lies in the region with black, dark grey to greenish shales with interaction of limestones & quartzites along with grey greenish phyllites with conglomerates & white massive quartzites in the upper parts. The upper slope at most of the sections consists of a thick layer of ill-sorted, loose, fine to coarse colluviums consisting of red soil with cobbles and boulders, consisting of 50-60% loose, fine soil and the remaining cobbles and boulders.

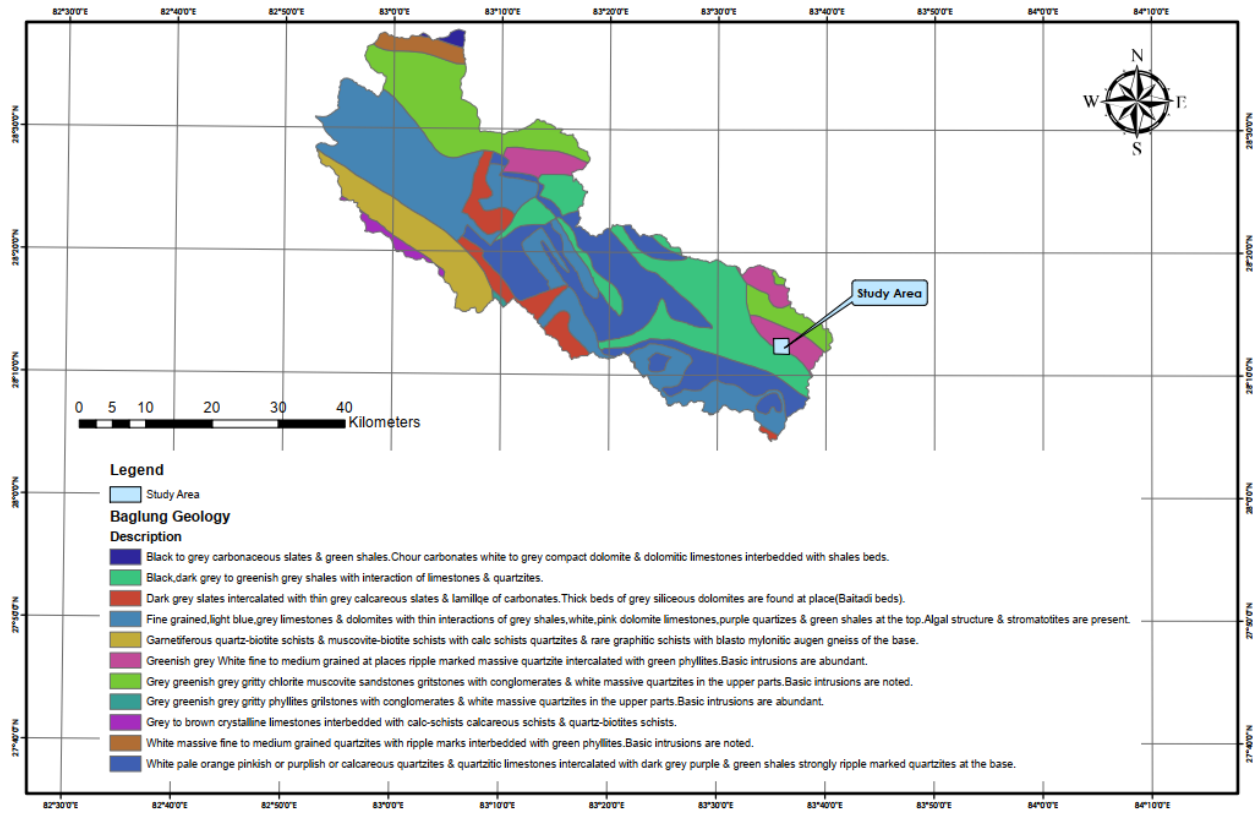

Figure 2: Geology of Baglung Municipality

2.2 Rainfall Conditions

The annual average rainfall distribution gradually decreases from the eastern to western regions of mountainous Nepal. The study area is located in the central region, where the annual rainfall is equal to the country's annual average. Rainfall data for this study were collected from the Department of Hydrology and Meteorology, Nepal. The rainfall recording station located within the study area, Baglung, was used.

Table 1: Meteorological station details

SN	Station name	Station No	Latitude	Longitude	Altitude, m
1	Baglung	605	28°15'49.407"N	83°36'9.258"E	964

The recorded rainfall at the stations shows that the maximum daily rainfall from 1980 to 2023 is 442.5 mm (Department of Hydrology and Meteorology, Daily Rainfall Records). This study considers the combination of intensity and duration of threshold rainfall for landslides in the region and the worst observed rainfall, 442.5 mm, in the study area for the debris flow event.

2.3 Landslides and Geotechnical Characteristics in the Study Area

Based on visual observations at the site, the area is covered with colluvial deposits and residual soil deposits on the slope. The formation of residual soil is determined by weathering the phyllite. Thick layers of the residual soil and colluvial deposits are seen around the slide area of Ramtola village.

The composition and orientation of the bedrock on the hill slope are the main causes of the slide's occurrence. Along the road alignment on the right side of the Ramtola slide, deep weathering of the phyllite can be seen in the field. Below the hill slope on the right side of the Ramtola slide, along the road section, a steep slope has also promoted instability. In the crown part of the slide, just below the road alignment, bedrock, along with residual soil, is present.

3 Methodology

3.1 Debris Flow Analysis

The initial position of the landslide and the spreading topography of the research region are necessary for the debris flow runout simulation. Empirical methods are preferable for modeling work with limited knowledge on the entire area, even if semi-empirical and dynamic methods can also be used to do the debris flow runout study. (Horton et al., 2013; Carrara et al., 2008; Finlay et al., 1999; O. Hungr, 1984). The Flow-R model, the susceptibility map, and empirical methodologies were taken into consideration in this study in order to determine the landside initiation site (source area). The model can be applied to debris flows for both runout and susceptibility studies. Applying the Flow-R model has produced reasonable results in a number of global locations. The program is publicly available and open-source. This model has a number of available algorithms. Figure 3 illustrates the established modeling process using Flow-R algorithms for debris flow runout. In this model, landslide source maps are applied to the runout analysis in Flow-R after being transformed by GIS software into an ASCII file format. The area map is used in GIS to compile the final Flow-R results. The regions where debris flows spread and landslides begin are depicted on the final map.

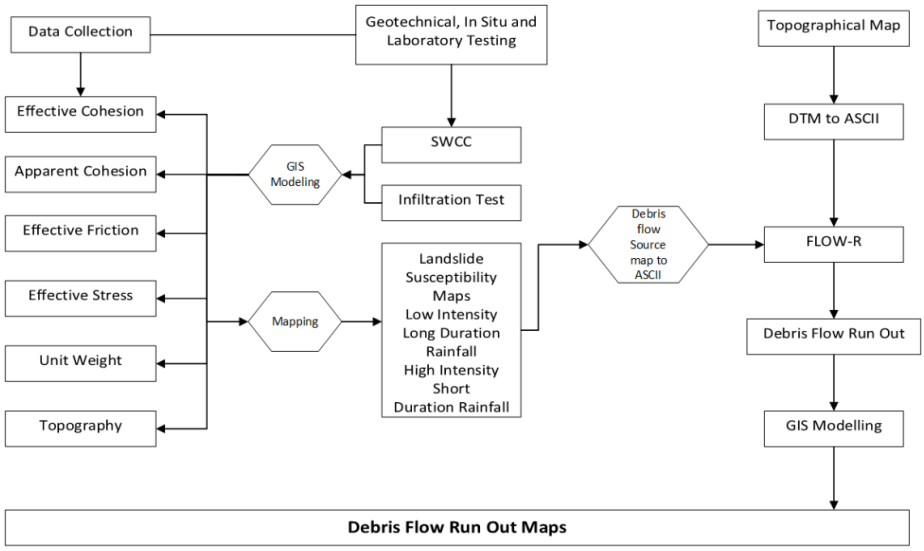

Figure 3: Modelling Procedure for debris flow

3.2 Spreading algorithms

To find the right algorithms for the study watershed, the debris flow runout distance, including spreading, was calculated using several algorithms mentioned in Table 2 (Flow-R model). The Flow-R model can be used to identify debris flow runout along with user-defined sources or landslide susceptibility and runout. All of these algorithms in Table 2, including the updated Holmgren (1994) model created by Horton et al. (2013), was run through the Flow-R model to determine which ones were most suited for this area. The best algorithms were used for the debris flow analysis of the entire watershed after the various algorithms were tested and validated.

The elevation of the center cell in the modified (Holmgren, 1994) model Table 2, Equation(1) is raised at the central location by a certain height (dh). The updated (Holmgren, 1994) model was used for single and multiple flow directions to two debris flow events that occurred outside the watershed but within Nepal's middle hills region. Claessens et al. (2005) investigated the exponent x in Equation (1) and determined that the range of 4 to 6, as proposed

by (Holmgren, 1994; Jaboyedoff et al., 2011) was an adequate value for spreading debris flow. In order to determine the proper value for debris flow inundation, a landslide of choice was tested with all conceivable x values ranging from 1 to 50.

$$\mathrm{P}i^{\mathrm{fd}} = \frac{(\tan Bi)^x}{\sum_{j=1}^{8}(tab\ Bj)^x} \ \forall \begin{cases} \tan B > 0 \\ x\varepsilon\ [1; +\infty] \end{cases} \qquad (1)$$

where i and j represent the flow directions, Bi and Bj the slope angles at the center cell in the i and j directions, and i the susceptibility proportion for the i direction. The range of exponent x is 1 to infinity. A multiple flow with decreasing direction and increasing value of x is represented when x equals 1.

For the eight directions of flow, O & Mark, (1984a) created Algorithm D8 Table 2. A comparison is made between the observed debris flow and the outcomes of all algorithms listed in Table 2, including the D∞ (D infinite) algorithm (Tarboton, 1997a) and the multiple flow direction technique (Quinn et al., 1991; Freeman, 1991).

Slope direction in natural terrain often varies, and a function must capture the new direction with regard to the initial slope. (Horton et al., 2013) refer to this function as the persistence function. The persistence function as provided in the Equation (2)was utilized by (Horton et al., 2013) and Gamma (2000) to determine how the slope direction changed in relation to the original or previous direction.

$$p_i^P = W_{\alpha(i)} \qquad (2)$$

where $W_{\alpha(i)}$ and $\alpha(i)$ are the angles from the preceding flow direction, and P_p^i is the flow percentage in the *i*-direction based on the weight and inertia of flow. There will not be any flow in the 180° angle opposite the previous flow direction in the ensuing stage. The weights of the persistence functions for debris flow propagation and inundation based on the initial direction can be determined using one of three methods for direction memory: (1) proportional (the software's default option), (2) cosine, or (3) (Gamma, 2000) Directions of 0 degrees, 45 degrees, and 90 degrees are assigned weights of 1, 0.8, and 0.4 by proportional, but directions of 135 degrees and 180 degrees have weights of zero. According to the cosines approach, the weights for the 0 and 45-degree orientations are 1 and 0.707, respectively, while the weights for the remaining 90, 135, and 180 degrees are equal to zero. Similarly, the Gamma, (2000) method assigns weights of 1.5 in the direction of flow (0 degrees), 1 for 45, 90 and 135 degrees, and zero for 180 degrees. The direction algorithms and persistence algorithms can be written as shown in Equation (3) (Horton et al., 2013).

$$p_i = \frac{p_i^{fd} p_i^p}{\sum_{j=1}^{8} p_i^{fd} p_i^p}\ p_o \qquad (3)$$

where i and j are the flow directions, p_i is the susceptibility value in direction i, P_p^i, is the flow proportion according to the flow direction algorithm, P_p^i is the flow proportion according to the persistence and P_o is the previously determined susceptibility, which is the total initial value or value of the central cell.

The susceptibility functions in the initial cell with p_o will be at their maximum and dispersed along the i and j flow directions. The probable direction of flow movement's potentiality is equal to, or not greater than, the total with the initial value of the central cell, which prevented and balanced the loss of susceptibility in the potential direction of flow cell. The susceptibility may persist until the debris flow's energy balance is disrupted.

Table 2: Available algorithms for debris flow propagation

Source area selection	Spreading algorithms				Energy calculation			
	Direction algorithm		Initial algorithm		Friction loss function		Energy limitation	
Only superior sources (Debris flows only), Energy base discrimination complete propagation of all source areas (long)	Holmgren -1984	Exponent 1 to 50	Weights	Default, cosinus, Gamma, 2000	Perla et al., 1980	Md 0010 to 7500 mu = 0.01 to 0.5	Velocity	1 mps to 50 mps
					Perla et al., 1980 No correction			
			Direction memory	Len = 005 to 100, Open 090 to 300	Travel angle Variable travel angle	From 0.1° to 50°		
	Holmgren, 1994 modified	Dh from 0.25 m to 70 exponents 0.1 to 50						
	D8	70 exponents 0.1 to 50						
	D Infinity (Freeman, 1991)							
	P. Quinn, 1991							
	Wichmann and Becht-2003	Threshold 10 to 50, exponent 1 to 50						
	Gamma, 2000	Threshold 10 to 50, Exponent 1 to 50						
	Rho8	-						

3.3 Debris Flow Travel Distance

In the Flow-R model, friction is the only cause of energy loss, and the flow mass is regarded as a unit value. The energy required to travel from one cell to another must be sufficient for flow to occur. Energy is the deciding element for both complete runout and spreading to side cells, according to (Horton et al., 2013) and as shown in the Equation(4) dependent on the difference between the delivered energy and available energy between two cells or cells around the central cell.

$$E_{kin}^{i} = E_{kin}^{0} + \Delta E_{pot}^{i} - E_{f}^{i} \qquad (4)$$

where $E_{kin}^{i}$is the kinetic energy of the cell in direction i, E_{kin}^{0} is the kinetic energy of the central cell, ΔE_{pot}^{i} is the change in potential energy to the cell in direction I and E_{f}^{i} is the energy lost in friction to the cell in direction i. Two different types of algorithms can be used to evaluate the friction loss: the simplified friction-limited model (SFLM) and the two-parameter friction model developed by (Perla et al., 1980) Depending on the parameters chosen, both approaches may produce comparable propagation regions (Jaboyedoff et al., 2011) Similar to snow avalanches, debris movement can be simulated using Voellmy's Equation (5).

$$T = A_i[\gamma H_i \left(cos\alpha + \frac{a_c}{g}\right) tan\,\emptyset + \gamma \frac{v_i^2}{\in} \qquad (5)$$

In this equation, T is a flow resistance, which is the function of the friction term and the turbulent term $\emptyset$ the friction angle, a_c the centrifugal acceleration, a_c the slope angle, A_i the base area (ds * Bi, where ds is the length of the sliding mass base and Bi is its width).
There are acceleration-related dimensions to the turbulence coefficient, $\in$. The centrifugal acceleration (a_c) is determined by the path's radius *r* and the flow velocity *v*. For rockslide avalanches, this model yields a reasonable result (Körner, 1976) In a DAN model, Hungr, (1995) effectively applied the Voellmy model to debris flow analysis. The two-parameter friction model proposed by Perla et al. (1980) and tested by Zimmermann was used for the analysis in this case, much like the Voellmy model. The momentum equation proposed by Perla et al. (1980) is taken into consideration for deriving the approach, which is based on a non-linear friction law (Horton et al., 2013) and is expressed by Equations (6)-(8).

$$v_i = (aiw(1 - exp\,bi) + v_o^2\ exp\,bi)^{1/2} \qquad (6)$$

$$a_i = g(sin\,Bi - \mu\, cos\,Bi) \qquad (7)$$

$$b_i = \frac{-2\,L_i}{w} \qquad (8)$$

where μ is the mass-to-drag ratio, a_i and b_i are fitting parameters, v_i is velocity in i direction, and μ is the friction parameter (Perla et al., 1980). The segment's length is denoted by L_i, its slope angle is *Bi*, its acceleration due to gravity is g, and its initial velocity is represented by v_o. A correction factor based on the conservation of linear momentum can be used, as shown in Equation (9), when the slope of the terrain drops quickly.

$$V_i' = V_i\, cos(B_i - B_{i+1}) \qquad (9)$$

The cosine of the angle difference between B_i and B_{i+1} times the initial velocity is represented by V_i' ' in Equation (9). More DEM space outside the connected processing cells is needed to accommodate the data for this correction factor. The algorithms in Flow-R allow for the consideration of large numbers of cells ((Horton et al., 2013). Corominas proposed the simplified friction limited model (SFLM), which is also available in Flow-R. It is predicated on the maximum runout distance that may be achieved by a tiny travel angle, as specified by Equation (10).

$$E_i^f = g\Delta x \, tan\emptyset \qquad (10)$$

where g is the acceleration brought on by gravity, tan∅ is the energy gradient in the direction of i, Δx is the horizontal displacement increment in direction i, and E_i^f is the energy lost in friction from the central cell to the cell in direction i.

For a realistic strategy, (Horton et al., 2013) recommended limiting the energy when there are steep slopes and high spreading or propagation. In order to limit the velocity from the provided value, they created Equation (11).

$$V_i = min\left\{\sqrt{(V_o^2} + 2g\Delta h - 2g\Delta x \, tan\,\emptyset)\,, V_{max}\right\} \qquad (11)$$

where V_{max} is the specified velocity limit and Δh is the height difference between the center cell and the cell in direction i. The user can set this limit according to the area. In general, $V_i$can only have a value that is between V_{max} and the intermediate value found in the first section of Equation (10). To cap the velocity and restrict propagation on steep slopes, the maximum velocity might be added. When evaluating the hazards in a region with a specific velocity condition, the model can be helpful.

3.4 Landslide Susceptibility Maps

A hazard map will be prepared based on the geological, engineering geological and geophysical results. The map will show that the high hazard zone is distributed at the middle part (source area) and along the gulley at the downslope area.

The data for the area were collected, including in situ and laboratory testing, from an old landslide site within the area. The soil strength parameters, such as cohesion, friction, and soil permeability, as well as results from the in-situ testing and laboratory results, will be utilized in the analysis.

A Digital Elevation Model (DEM) was used to develop other required maps, such as a slope map of the area. All maps, including suction, density, friction, cohesion, and infiltration depth characteristics, were developed in the GIS environment. These maps were interpolated with Inverse Distance Weighted (IDW) methods to create the raster maps. The same cell size and boundary extent were applied in the raster analysis. Further, the result from the Flow-R analysis will also be incorporated as the maximum probable flow to derive the susceptibility map.

4 Results and Discussions

4.1 Comparison of The Predicted Debris Flows Runout Areas with Observed Debris Flows Runout Areas in The Study Region

The observed source and debris flow inundation areas were collected for the study. In Table 2, source area selection, spreading algorithms, and control mechanisms or energy control are given in separate columns and can be selected individually. Any combination of all alternatives from each column and sub-column can be applied to model debris flow. All these choices were applied to identify a debris flow model for the study region. The debris flow area predicted by using all algorithms was then compared with the three observed areas shown in Figure 4, and a debris flow area is selected for modelling.

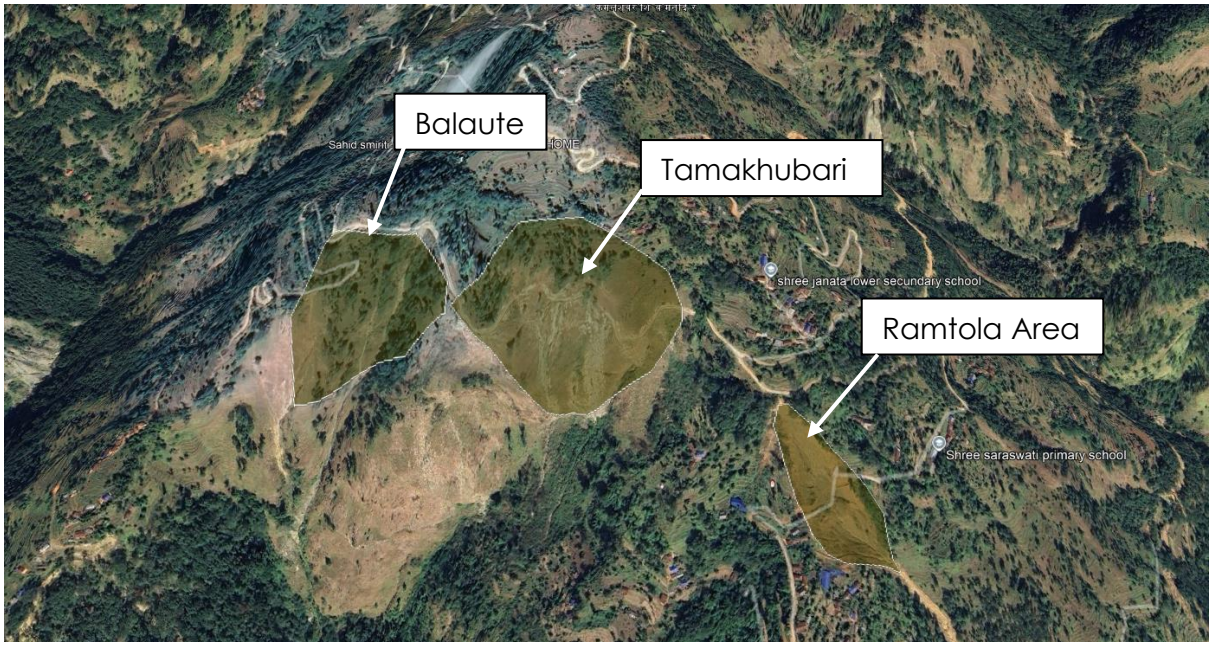

Figure 4: Landslide Area selection for modelling

4.1.1 Area Selection for Modelling

A total of three areas were initially chosen as suitable for modeling. Among these, the Ramtola landslide, located at 28° 12' 00" N, 83° 36' 00" E, with an average elevation of 1260 m above mean sea level (masl) Figure 4, within the Baglung Municipality of Baglung District, Nepal, was chosen for detailed Flow-R modeling due to the availability of historical landslide records and topographical survey data

4.1.2 Algorithm for Modelling

The algorithms presented in Table 2 were applied to the Ramtola landslide to predict the debris flow spreading area. The observed debris flow spreading outline for the Ramtola landslide is shown in Figure 5. The three available options for source selection in column 1 of Table 2, ‘‘Only Superior Sources (Debris-Flows Only),’’ ‘‘Energy Base Discrimination’’ and ‘‘Complete Propagation of all Source Areas (long),’’ all provided similar results; no difference was observed by choosing any of these three methods. All combinations of column 2 and its sub-column and column 3 and its sub-column in Table 2 were applied in the analysis or modelling of debris flow spreading. Propagation was not observed using D8, Rho8, and D-infinity with all other combinations. Similarly, other algorithms with large travel angles also did not produce the observed debris flows. Moreover, the (Freeman, 1991) model or algorithm, Table 2, was tested with the observed debris flows, but the result found only small spreading. Therefore, these algorithms were not applied to predict debris flow spreading areas in the study watershed. For instance, the result of the analysis for the D8 algorithm (O & Mark, 1984b) found no spreading, similar to the results found by (Desmet & Govers, 1997), (Endreny & Wood, 2003) (Tarboton, 1997b) and (Tarboton, 1997). Tarboton (1997b) proposed the D∞ (D infinity) algorithm, which was also used for the analysis of the observed debris flows, but the spreading was small, as also found by Horton et al. (2013). (Fairfield, 1991) proposed the Rho8 algorithm, a stochastic method, but the result was unable to capture the observed debris flow location, similar to the findings of (Erskine et al., 2006).

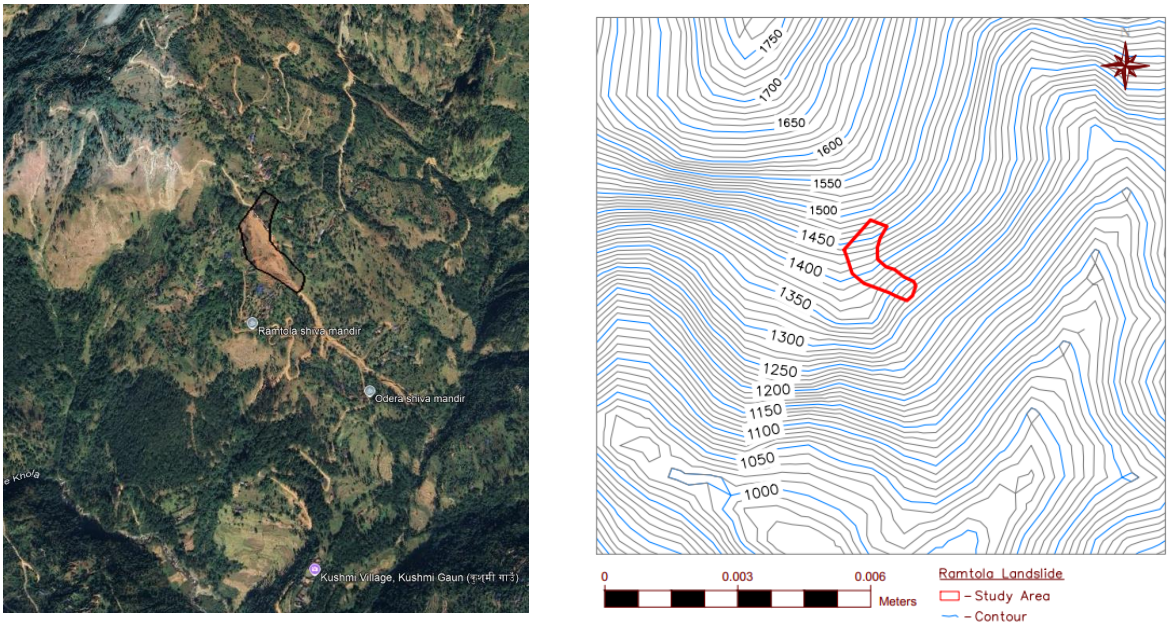

Figure 5:Observed debris flow (study area)

4.1.3 Comparison

The multiple flow direction algorithm or model proposed by (P. Quinn, 1991) provided satisfactory results compared to those observed in the field. In other words, the debris flow spreading area for the Ramtola landslide predicted by using (P. Quinn, 1991)'s algorithm is relatively similar to that observed in the field. Similar satisfactory validation results were also obtained when the (Holmgren, 1994)'s or (Gamma, 2000)'s or ''Weights'' and ''Cosinus'' initial algorithms were used as evidenced by Figure 6 shows that the modeled or predicted debris flow spreading (by using (Holmgren, 1994)'s model) is similar to the observed debris flow. Therefore, the modified (Holmgren, 1994) algorithm was applied for the simulation or prediction of debris flows in the study watershed, Ramtola. This will provide a more conservative spreading area, which is more suitable with respect to debris flow or landslide hazards and risk evaluation.

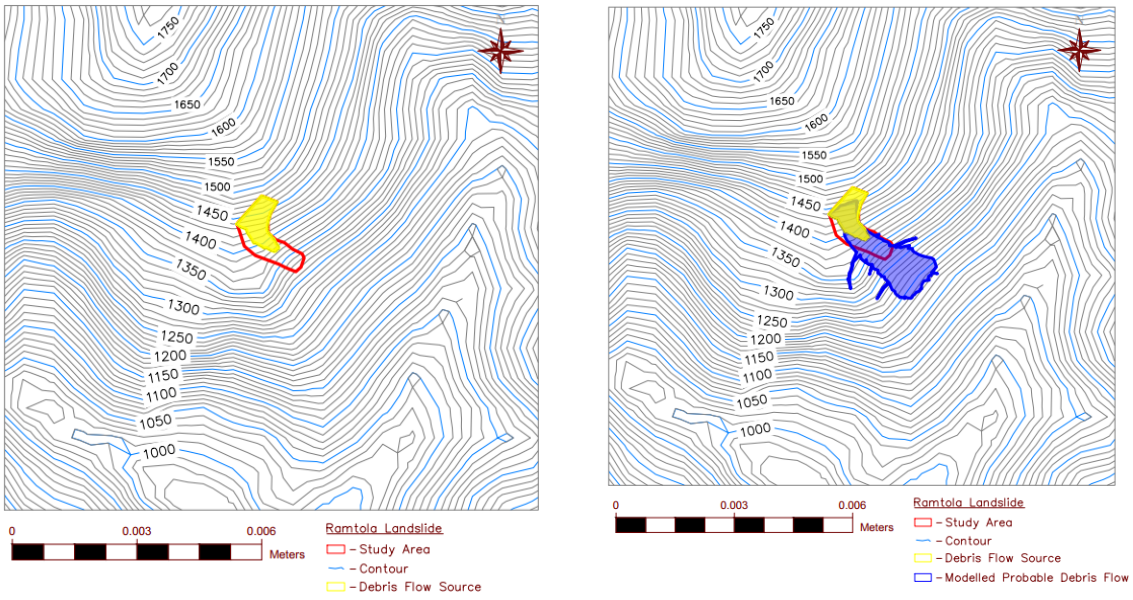

Figure 6: Modeled or predicted debris flow outline vs observed debris flow (study area) outline for the Ramtola landslide

4.2 Landslide Susceptibility Mapping

4.2.1 Field-based susceptibility mapping

Based on the site assessment, a geological map was created, incorporating engineering geology and the current terrain. The area at the top of the landslide, which is the source of the slide, consists of significantly weathered rock mixed with colluvial deposits. These deposits are composed of red soil, cobbles, and boulders, as detailed in Figure 7.

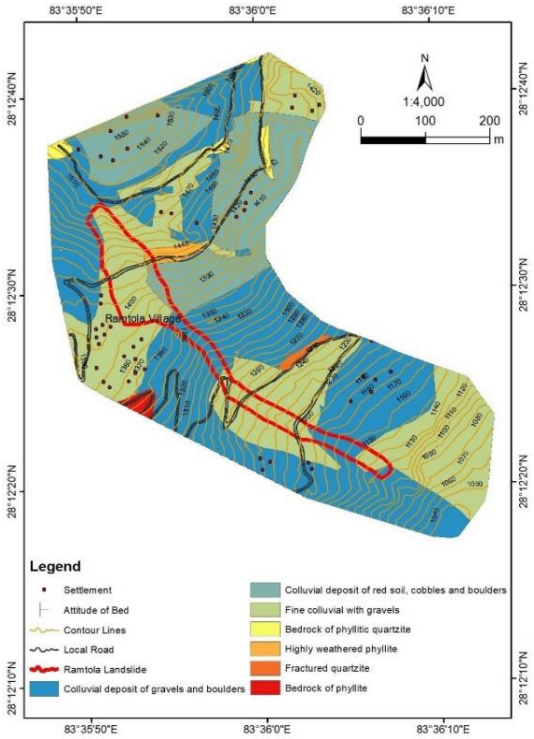

Figure 7: Geological map as per site condition

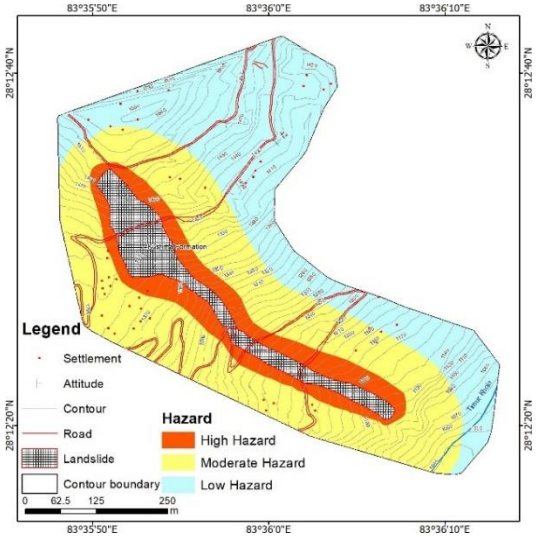

Figure 8: Field Based Hazard Map

To determine areas susceptible to landslides and assess the severity of the hazard, a separate hazard map was generated. This process involved integrating various datasets, including

topographical survey information, land use and land cover data, and existing maps of the area. By combining these diverse spatial datasets, areas with a higher propensity for landslides and varying degrees of potential impact can be identified and mapped in the resulting hazard map.

Figure 9 illustrates a Landslide Susceptibility Map developed through field-based investigations. This map provides a visual representation of the potential landslide occurrences across the study area, informed by direct on-site observations and thorough assessments of the specific geological, geomorphological, and hydrological characteristics. The susceptibility map generated through this direct, ground-level evaluation then served as a critical benchmark for comparison against the results obtained from other alternative approaches.

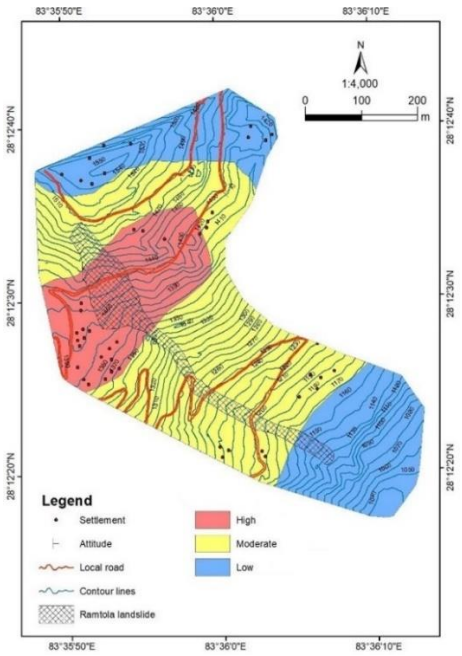

Figure 9: Field-based landslide Susceptibility Map

4.2.2 GIS-based Susceptibility Mapping

The relevant factors are selected and assigned weights reflecting their influence on landslide occurrence, by statistical analysis of past landslide events. Within the GIS environment, these weighted raster layers are overlaid using cell-by-cell operations, commonly through a weighted overlay method. This process combines the values of corresponding cells based on their assigned weights to generate a continuous landslide susceptibility index. This index is then classified into discrete susceptibility zones, visually represented on a map with a clear legend. Finally, the accuracy and reliability of the resulting susceptibility map are assessed through validation against independent datasets or field observations, ensuring its utility for land-use planning and risk mitigation efforts. Focusing on specific study areas, the results obtained including the slope map, elevation map, aspect map, and curvature map, as shown in Figure 10.

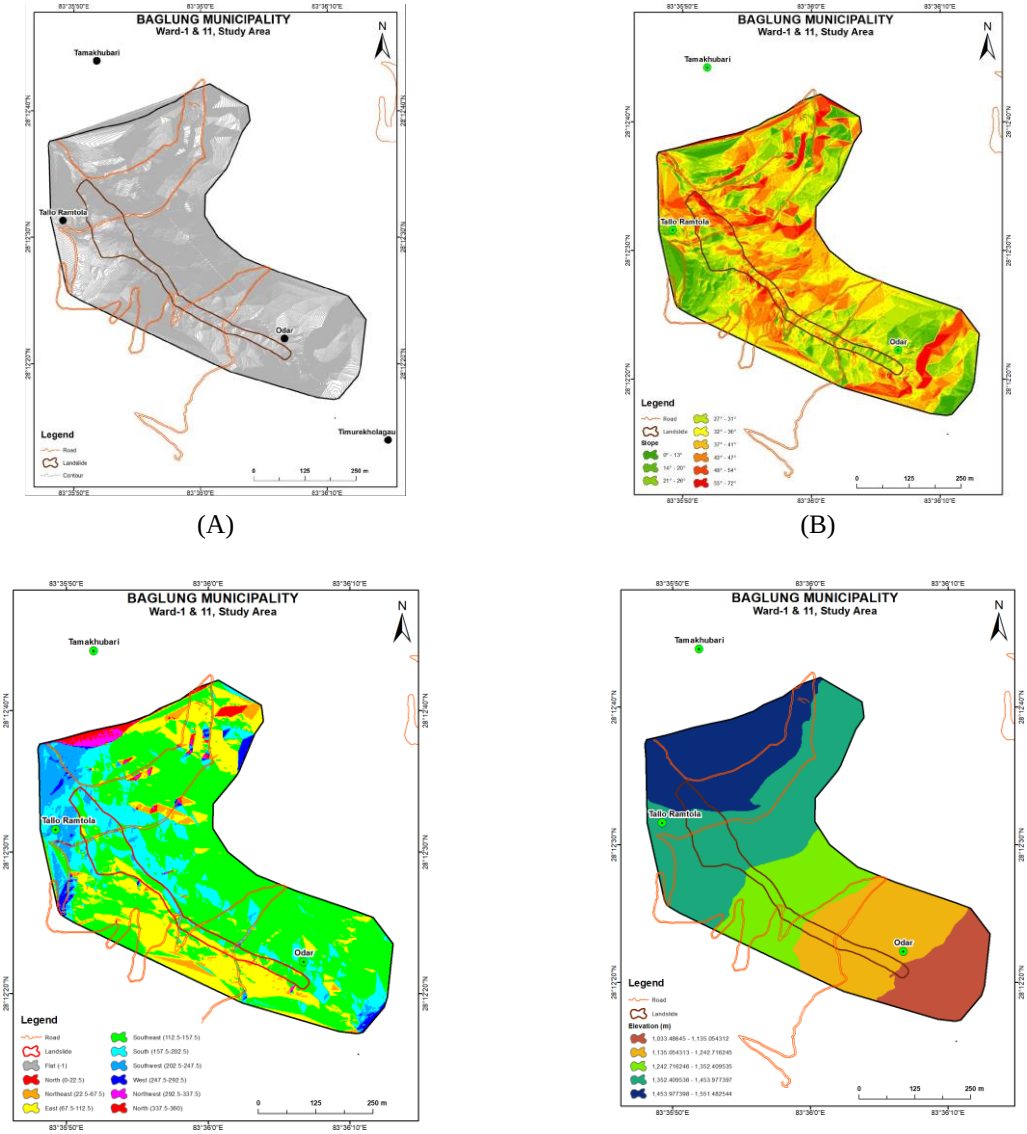

Figure 10: (A)Topography, (B)Slope, (C)Aspect, (D)Elevation map of Ramtola

4.2.3 Flow-R Generated Susceptibility Mapping

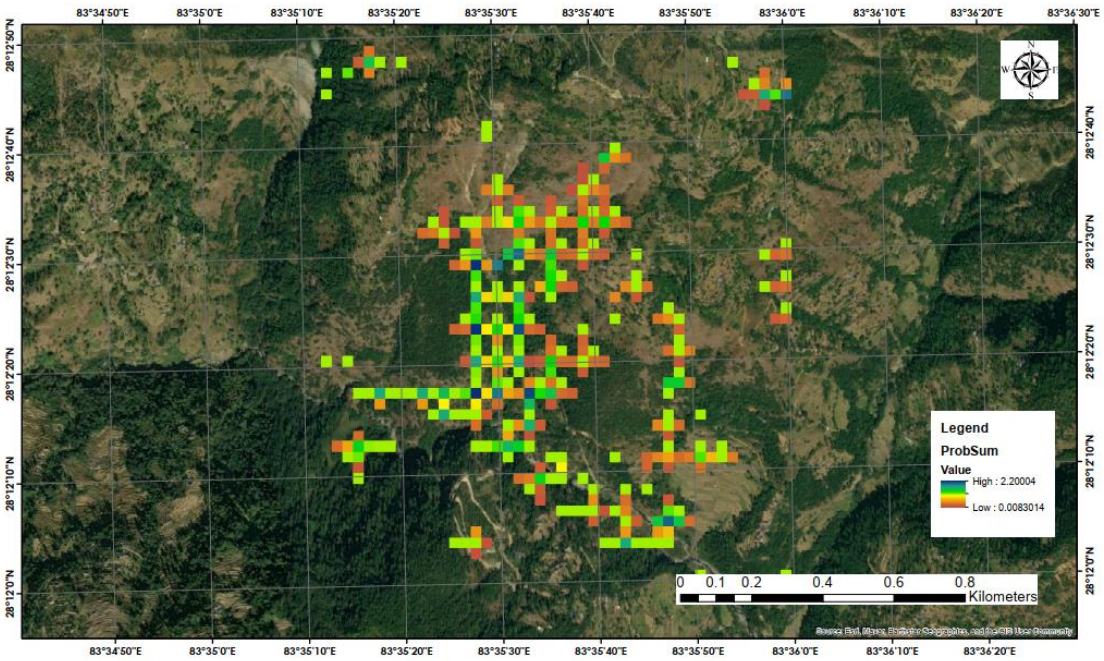

Figure 11: Susceptibility map generated from Flow-R

Flow-R's methodology involves simulating landslide movement using physical or empirical models based on friction laws (e.g., Voellmy, Coulomb-Viscous) and topographic steering dictated by the underlying Digital Elevation Model. By simulating multiple scenarios with varying parameters, Flow-R can generate outputs such as runout probability or inundation frequency, highlighting areas susceptible to being impacted by moving landslides. These Flow-R outputs are integrated with initiation susceptibility maps through GIS overlay techniques, such as cell-by-cell combination or weighted averaging, to create a comprehensive susceptibility map. This integration allows for a holistic understanding of landslide hazards, considering both the likelihood of initiation and the potential extent of runout.

For input parameters required for Flow-R test pits were dug in the landslide area to perform the laboratory testing which determines soil strength parameters, such as cohesion, friction, and soil permeability. Figure 11 shows the susceptibility map generated from Flow-R, with max probability ranging from the lowest 0.008 to the highest of 2.20.

4.2.4 Combined Susceptibility Mapping

Employing a frequency ratio method, a landslide susceptibility index map was generated by integrating five key parameters: Land Use Land Cover, Distance from Road, Flow Direction, Relief, and Slope. Analysis of this map revealed that the area surrounding the Ramtola landslide falls within the very high susceptibility zone, indicating a significant propensity for future slope failures. Furthermore, the maximum likely flow and susceptibility map produced using the Flow-R model, as depicted in Figure 11, was integrated with the field-based susceptibility map Figure 9 and the GIS-based assessment illustrated in Figure 10.

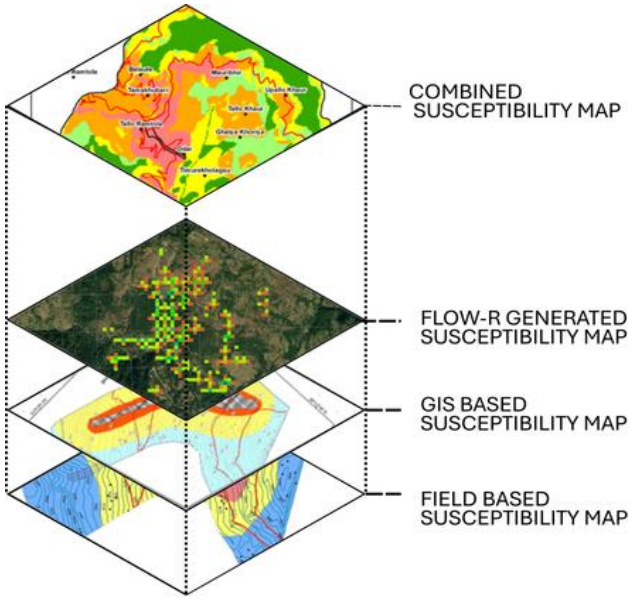

Figure 12: A framework to combine the maps

These three independent datasets were subsequently interpolated to derive the combined susceptibility map. The framework to generate this has been shown in Figure 12.

To create a comprehensive landslide susceptibility map across the entire region, the results from all three methodologies were interpolated and combined to form a final, integrated susceptibility map. This process involved an initial sampling of a smaller portion of the study area using the field-based and GIS-based methods, the results of which were then overlaid and harmonized with the susceptibility patterns generated by the Flow-R model. These datasets' subsequent interpolation and combination yielded a spatially continuous assessment of landslide susceptibility for the entire region.

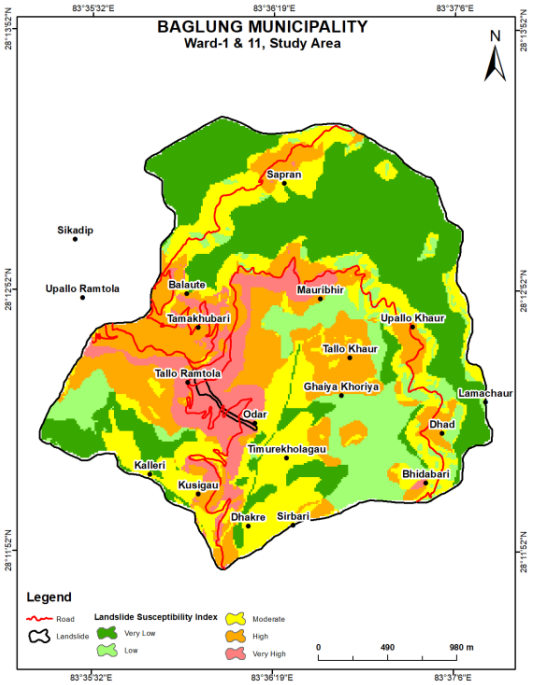

Figure 13: Susceptibility map of Ramtola

Figure 13 illustrates the resulting combined landslide susceptibility map for the Ramtola region. Analysis of this map indicates that the largest portion of the area (31%) is classified as having very low susceptibility, while the smallest portion (10%) is categorized as very high

susceptibility, the more detail of this is shown in Table 3. Specifically, the villages of Tallo Ramtola, Odar, and Kusigau are located within the very high susceptibility zone. The villages of Mauribhir, Dhad, Tallo Khaur, and Balaute are situated in areas of high susceptibility. Moderate susceptibility characterizes the zones encompassing Kalleri, Dharke, Sirbari, Timurekhola gaun, and Sapran. Finally, Lamachaur and Ghaiya Khoria are located within the low susceptibility zone.

Table 3: Area (%) occupied by different susceptible zones in the study area

LSI	**Value**	**Count**	**Area (m^2)**	**Area (km^2)**	**Percentage(%)**
Very Low	1	12718	2042587.85	2.04	31%
Low	2	5450	875303.02	0.88	13%
Moderate	3	9160	1471151.5	1.47	23%
High	4	9132	1466654.53	1.47	23%
Very High	5	3949	634233.326	0.63	10%
Total			6489930.22	6.49	100%

5 Conclusions

The Flow-R modeling provided potential runout pathways and inundation areas by validating against observed debris flow events of Ramtola. The model simulated by the modified (Holmgren, 1994) provided a more conservative spreading area, rather than other algorithms like P. Quinn, 1991 and Gamma, 2000. The model also provided hazard propagation beyond the initiation zones and derived susceptibility maps. The integrated susceptibility map, generated by combining field-based mapping, GIS-based analysis, and Flow-R modeling, produce a reliable framework for assessing debris flow hazards in mountainous terrain. The empirical method used by Flow-R has proven to be a highly effective tool for debris flow analysis in resource-limited countries like Nepal. Given the minimal data and resources available in such regions, Flow-R's open-source and user-friendly nature makes it an ideal solution for predicting debris flow paths and generating susceptibility maps for risk management.

6 Acknowledgment

The authors are thankful to the Department of Water Resources and Irrigation (DWRI), Vulnerable Landslide Management Project, Pulchowk, Nepal, and Explorer Geophysical Consultants Pvt. Ltd. for their approval and for providing the relevant documents to prepare this paper.

7 References

[1] Carrara, A., Crosta, G., & Frattini, P. (2008). Comparing models of debris-flow susceptibility in the alpine environment. *Geomorphology*, *94*(3–4), 353–378. https://doi.org/10.1016/j.geomorph.2006.10.033

[2] Claessens, L., Heuvelink, G. B. M., Schoorl, J. M., & Veldkamp, A. (2005). DEM resolution effects on shallow landslide hazard and soil redistribution modelling. *Earth Surface Processes and Landforms*, *30*(4), 461–477. https://doi.org/10.1002/esp.1155

[3] Dahal, R., Hasegawa, S., & Yamanaka, M. (2006). *Rainfall Triggered Flow-Like Landslides: Understanding from Southern Hills of Kathmandu, Nepal and Northern Shikoku, Japan*. https://www.researchgate.net/publication/255600544

[4] Desmet, P. J. J., & Govers, G. (1997). Two-dimensional modelling of the within-field variation in rill and gully geometry and location related to topography. In *P.J.J. Desmet, G. Govers / Catena* (Vol. 29, Issue 96).

[5] Du, J., Fan, Z. J., Xu, W. T., & Dong, L. Y. (2021). Research Progress of Initial Mechanism on Debris Flow and Related Discrimination Methods: A Review. In *Frontiers in Earth Science* (Vol. 9). Frontiers Media S.A. https://doi.org/10.3389/feart.2021.629567

[6] Endreny, T. A., & Wood, E. F. (2003). Maximizing spatial congruence of observed and DEM-delineated overland flow networks. *International Journal of Geographical Information Science*, *17*(7), 699–713. https://doi.org/10.1080/1365881031000135483

[7] Erskine, R. H., Green, T. R., Ramirez, J. A., & MacDonald, L. H. (2006). Comparison of grid-based algorithms for computing upslope contributing area. *Water Resources Research*, *42*(9). https://doi.org/10.1029/2005WR004648

[8] Fairfield, J. (1991). Drainage Networks From Grid Digital Elevation Models. In *WATER RESOURCES RESEARCH* (Vol. 27, Issue 5).

[9] Finlay, P. J., Ostyn, G. R. M., & Fell, R. (1999). *Landslide risk assessment: prediction of travel distance*.

[10] Freeman, T. G. (1991). Calculating Catchment Area with Divergent Flow Based on A Regular Grid. In *Computers & 6eosciences* (Vol. 17, Issue 3).

[11] Gamma, P. (2000). *dfwalk-Ein Murgang-Simulationsprogramm zur Gefahrenzonierung. Geographica Bernensia. G66. Diss. Naturwiss. Bern (kein Austausch). Literaturverz.*

[12] Holmgren, P. (1994). Multiple flow direction algorithms for runoff modelling in grid based elevation models: An empirical evaluation. *Hydrological Processes*, *8*(4), 327–334. https://doi.org/10.1002/hyp.3360080405

[13] Horton, P., Jaboyedoff, M., Rudaz, B., & Zimmermann, M. (2013). Flow-R, a model for susceptibility mapping of debris flows and other gravitational hazards at a regional scale. *Natural Hazards and Earth System Sciences*, *13*(4), 869–885. https://doi.org/10.5194/nhess-13-869-2013

[14] Hungr, O. (1995). A model for the runout analysis of rapid flow slides, debris flows, and avalanches. *Canadian Geotechnical Journal*, *32*(4), 610–623. https://doi.org/10.1139/t95-063

[15] Hungr, O., Leroueil, S., & Picarelli, L. (2014). The Varnes classification of landslide types, an update. In *Landslides* (Vol. 11, Issue 2, pp. 167–194). Springer Verlag. https://doi.org/10.1007/s10346-013-0436-y

[16] Jaboyedoff, M., Rudaz, B., & Horton, P. (2011). *Concepts and parameterization of Perla and FLM model using Flow-R for debris flow*. https://www.researchgate.net/publication/319314382

[17] Körner, H. J. (1976). *Reichweite und Geschwindigkeit von Bergstürzen und Fließschneelawinen. Rock mechanics, 8, 225-256.*

[18] O. Hungr. (1984). *Experiments on the flow behaviour of granular materials at high velocity in an open channel* (Vol. 34, Issue 3).

[19] O, J. F., & Mark, D. M. (1984a). *The Extraction of Drainage Networks from Digital Elevation Data* (Vol. 28).

[20] O, J. F., & Mark, D. M. (1984b). *The Extraction of Drainage Networks from Digital Elevation Data* (Vol. 28).

[21] P. Quinn. (1991). *The Prediction of Hillslope Flow Paths for Distributed Hydrological Modelling Using Digital Terrain Models* (Vol. 5).

[22] Perla, R., Cheng, T. T., & McClung, D. M. (1980). A two-parameter model of snow avalanche motion. *Journal of Glaciology*, *26*(94), 197–207. https://doi.org/10.1017/S002214300001073X

[23] Tarboton, D. G. (1997a). A new method for the determination of flow directions and upslope areas in grid digital elevation models. *Water Resources Research*, *33*(2), 309–319. https://doi.org/10.1029/96WR03137

[24] Tarboton, D. G. (1997b). A new method for the determination of flow directions and upslope areas in grid digital elevation models. *Water Resources Research*, *33*(2), 309–319. https://doi.org/10.1029/96WR03137

[25] Vianello, D., Vagnon, F., Bonetto, S., & Mosca, P. (2023). Debris flow susceptibility mapping using the Rock Engineering System (RES) method: a case study. *Landslides*, *20*(4), 735–756. https://doi.org/10.1007/s10346-022-01985-6

[26] Xu, H., Su, P., Chen, Q., Liu, F., Zhou, Q., & Liu, L. (2022). Susceptibility areas identification and risk assessment of debris flow using the Flow-R model: a case study of Basu County of Tibet. *Geoenvironmental Disasters*, *9*(1). https://doi.org/10.1186/s40677-022-00216-3